

Mass Function Gradients and the Need for Dark Matter

Accepted for publication in *The Astrophysical Journal Letters*

Jason A. Taylor^{1,2}

Department of Physics, United States Naval Academy, Annapolis, MD 21402-5026, USA; E-mail
(Internet): taylor@milkyway.gsfc.nasa.gov

ABSTRACT

There is both theoretical and empirical evidence that the initial mass function (IMF) may be a function of the local star formation conditions. In particular, the IMF is predicted to flatten with increasing local luminosity density ρ_l , with the formation of massive stars being preferentially enhanced in brighter regions. In R136, the bright stellar cluster in 30 Doradus, the IMF gradient is $\partial\Gamma/\partial\log\rho_l = 0.28 \pm 0.06$, where Γ is the slope of the IMF. If such IMF gradients are indeed general features of galaxies, this implies that several previous astrophysical measurements, such as the surface mass densities of spirals (obtained assuming constant mass to light ratios), were plagued by substantial systematic errors. In this Letter, calculations which account for possible IMF gradients are presented of surface densities of spiral galaxies. Compared to previous estimates, the mass surface densities corrected for IMF gradients are higher in the outer regions of the disks. For a model based on the Milky Way but with an IMF scaled according to R136, the rotation curve without the traditional dark halo component falls with Galactocentric radius, though slower than it would without IMF gradients. For a second model of the Milky Way in which the IMF gradient is increased to 0.42, the rotation curve is approximately flat in the outer disk, with a rotational velocity below $\simeq 220 \text{ km s}^{-1}$ only before the traditional dark halo component is added. For a third model in which substantial arm/interarm density contrasts are additionally assumed, the solar vicinity mass density drops to $0.10M_\odot\text{pc}^{-3}$, which is consistent with observations. These results, if generalizable to other galaxies, not only call into question the assertion that dark matter halos are compatible with the flat rotation curves of spiral galaxies, but also may clarify our understanding of a wide variety of other astrophysical phenomena such as the G-dwarf problem, metallicity gradients, and the Tully-Fisher relation.

Subject headings: galaxies: luminosity function, mass function — galaxies: kinematics and dynamics — dark matter — galaxies: halos — Magellanic Clouds — galaxies: evolution

¹Postal address: NASA/GSFC, Laboratory for High Energy Astrophysics, Code 661, Greenbelt MD 20771, USA

²Department of Physics, University of Maryland, College Park, MD 20742, USA

1. INTRODUCTION

In a recent paper, Padoan, Nordlund, & Jones (1997) claimed on theoretical grounds that the initial mass function (IMF) should be a function of the local temperature T of the original molecular clouds. Padoan et al. (1997) argued that dense star forming regions, such as those in starburst galaxies, should be warmer than sparser star forming regions. In fact, if the temperature dependence of the clouds is not drastically different from that of a blackbody, then $T \propto \rho_1^{1/4}$, where ρ_1 is the local mean luminosity once star formation has already started. Padoan et al. claimed that starburst regions should therefore have a flatter IMF and be more “top heavy.” Similar reasoning would imply that the IMF in cooler regions of galaxies should favor low mass star formation and be steeper.

In support of their star formation model, Padoan et al. (1997) noted that for $T \gtrsim 60$ K, their models predict a top heavy IMF similar to that found in the center of R136 (Malumuth & Heap 1994, Brandl et al. 1996), the bright stellar cluster in 30 Doradus. Due to its proximity and the fact that it is the most massive H II region in the Local Group, 30 Doradus is perhaps the best star formation “laboratory” accessible to us. However, the relaxation time in R136 may be less than its age (Campbell et al. 1992), so dynamic friction may also contribute toward the R136 present-day mass function gradient.

Fortunately, many other avenues of testing Padoan et al.’s model exist. The O-star catalog of Garmany, Conti, & Chiosi (1982) shows a flattening of the IMF slope toward the Galactic center (cf Humphreys & McElroy 1984). This data supports Padoan et al.’s model since higher surface brightness regions would, on the average, yield higher temperatures and flatter IMFs. Models which attempt to explain correlations between local surface brightness, color, line ratios, metallicity, and the star formation rate have assumed luminosity-dependent IMFs (e.g., Edmunds & Phillipps 1989; Phillipps, Edmunds, & Davies 1990). Several evolutionary models of inner regions of starburst galaxies assume low mass cutoffs or top heavy IMFs (e.g., Rieke et al. 1980; Augarde & Lequeux 1985; Doane & Mathews 1993; Doyon, Joseph, & Wright 1994). Finally, independent theoretical arguments supporting IMF gradients range from models which are consistent with the simple form of the Jeans expression for the typical stellar mass in solar units of $\langle m \rangle \propto T^{3/2}$ (e.g.; Larson 1982; Bodenheimer, Tohline, & Black 1980) to much more complicated models, such as the outflow-regulated model of Adams & Fatuzzo (1996), which predicts $\langle m \rangle \propto T^a$, where $1 \leq a \leq 3/2$.

If IMFs are actually a function of ρ_1 or T , there would be several important astrophysical consequences. For instance, there would be a position-dependence in the mean mass to light ratio. This is due to the strong dependence of the mass to light ratio upon the IMF. In R136, this makes the mass density function ρ_m much different from ρ_1 (Malumuth & Heap 1994, Brandl et al. 1996) and complicates estimates of the total mass. Padoan et al.’s results indicate that similar effects might occur in spiral galaxies. If the luminosity of a star is taken as $L \simeq L_\odot m^y$, where $y \simeq 3.5$, the Jeans expression above would suggest the crude relation $\langle m \rangle \propto \rho_1^{3/8}$ and yield $\rho_m \propto \rho_1^{1+3(1-y)/8} \simeq \rho_1^{0.06}$. Unfortunately, previous works have assumed that IMFs are independent of time and position with,

specifically, $\rho_m \propto \rho_1^{1.0}$ throughout a given spiral galaxy (e.g., van Albada et al. 1985). In this *Letter*, surface mass densities of spiral galaxies are computed, for the first time, by explicitly accounting for the possible types of IMF gradients that might exist if theories like those of Padoan et al. are correct.

2. AN EMPIRICAL ESTIMATE OF THE R136 IMF GRADIENT

Since position-dependent measurements in R136 of both ρ_1 and the IMF slope Γ (where $dN/dM \propto m^{\Gamma-1}$ is the number of stars per unit mass in solar units) have already been made, computing the dependence of the R136 IMF upon the local luminosity is straightforward. Doing this will provide a useful starting point in obtaining a crude yet quantitative estimate of the possible types of IMF gradients that might generally exist in all galaxies including the Milky Way.

Table 1 summarizes Brandl et al.’s (1996) results for the IMF based upon high resolution 5-color photometry of the stars in R136 estimated to be between 2.5 and 3.5 Myrs years old. The right-most entry of Table 1 shows the results of performing the coordinate transformation between R and ρ_1 using Figure 15 of Hunter et al. (1996). Though Brandl et al. (1996) did not make explicit measurements of the upper and lower stellar mass cutoffs m_l and m_u to the power-law approximation of the IMF, Table 1 includes estimates of their dependences upon the local surface brightness. The lower mass limits were obtained from the peaks of Brandl et al.’s mass functions, while the upper limits were taken from the highest masses observed per radius bin. Both $\log_{10}(m_l)$ and $\log_{10}(m_u)$ are found to decrease by $\simeq 0.2$ with each successive increase in radius. Brandl et al. (1996) performed completeness corrections, so the depletion of low mass stars in all but the outer regions of R136 is presumably real. The results of performing a linear fit of the IMF parameters of R136 to $\log_{10}(\rho_1)$ are shown in columns 2-7 of Table 2 as Model A. Uncertainties of parameters calculated from more than two radius bins are shown in parenthesis.

3. DYNAMICAL PROPERTIES OF SPIRAL GALAXIES WITH IMF GRADIENTS

The IMF gradient of Model A implies a surface mass density that is different from what would be obtained were the mass to light ratio constant. The surface mass density for Model A, if scaled according to the surface luminosity function suspected for the Galaxy, is shown in the top panel of Figure 1. The disk scale length $R_0 = 4.5$ kpc and solar Galactocentric radius $R_\odot = 7.8$ kpc were taken from Kuijken & Gilmore’s (1989a) model of the Galaxy. For simplicity, ρ_1 at a given radius was assumed to be constant throughout a disk thickness of 575 pc. The surface brightness was normalized to be $22.5 L_\odot \text{pc}^{-2}$ at $R = R_\odot$, which results in $\rho_{1\odot} \equiv \rho_1(R_\odot) = 0.037 L_\odot \text{pc}^{-3}$. For each radius bin, the IMF was obtained from ρ_1 and the coefficients shown in Table 2 for Model A. This IMF was converted to present day mass and luminosity functions by assuming (purely

for simplicity) a constant star formation rate for the past 1.0×10^{10} yrs. The main sequence lifetime-luminosity-mass relationships used to obtain the mass to light ratio as a function of the IMF were obtained from logarithmic-linear interpolation of $m \geq 0.8$ models published by Schaller et al. (1992) for $z = 0.02$, overshooting of the $m \geq 1.5$ stars, and standard mass loss rates. For $m < 0.8$, $L|_{m=0.25} = 7.8 \times 10^{-4} L_{\odot}$, $L|_{m=0.08} = 6.55 \times 10^{-9} L_{\odot}$, and $L|_{m \leq 0.07} = 5.0 \times 10^{-12} L_{\odot}$ were assumed.

The surface densities both of Model A and of the constant mass to light ratio model fall off exponentially with increasing radius. The effective scale length of Model A is $\simeq 7.5$ kpc, which is $\simeq 1.7$ times larger than that of the surface brightness function. This increase in the scale length is a result of the fraction of low mass stars (and the mass to light ratio) increasing with radius.

From the surface density, other dynamical properties of the galaxy can also be calculated. The circular velocity (i.e., the rotation curve) corresponding to the surface density of Model A is shown in the second panel of Figure 1. The parameters for the bulge, spheroid, and halo were taken from Table 1 and Figure 5 of Kuijken & Gilmore’s (1989a) model of the Galaxy. To avoid a divergent and unphysical total mass, the additional assumption that all components of the Galaxy terminate at an arbitrarily-selected maximum radius of 35.0 kpc was also made. For Model A, this results in a total mass of the halo, bulge/spheroid, and disk of, respectively, $2.8 \times 10^{11} M_{\odot}$, $3.5 \times 10^{10} M_{\odot}$, and $6.3 \times 10^{10} M_{\odot}$. In comparison, the integrated disk mass of the $\gamma_V = 2.0 M_{\odot}/L_{\odot}$ model is only $3.2 \times 10^{10} M_{\odot}$ and increases much faster with radius. For simplicity, the surface mass density of stellar remnants and gas was assumed throughout the disk to be 1/3 that of the stars. Because the halo dominates the mass distribution, the circular velocity curve (solid line) is nearly flat. Without the halo, the circular velocity curve falls from 185 km s^{-1} at $R = 2.0$ kpc to 124 km s^{-1} at $R = 34$ kpc. Though the surface density of Model A corrected for IMF gradients is different from that previously obtained for spiral galaxies, Figure 1 shows that the change is not enough to dramatically affect the dynamical properties of the disk, such as the circular velocity curve.

The IMF of Model A is very negative at all radii, with $\Gamma|_{R=1.0 \text{ kpc}} = -3.2$, $\Gamma|_{R=R_{\odot}} = -3.4$, and $\Gamma|_{R=15.0 \text{ kpc}} = -3.6$. This occurs even though R136’s spatially-averaged IMF is typical and its IMF gradient is small only because it has a luminosity density that is $\sim 10^4 - 10^8$ times higher than typical regions of spiral galaxies. For comparison, Miller & Scalo (1979) obtained much higher values of $\Gamma = -0.4, -1.5$, and -2.3 for, respectively, $0.1 < m < 1.0$, $1.0 < m < 10$, and $m > 10$. This suggests that R136’s IMF is correlated with ρ_1 in a somewhat different way than the correlation that might exist in the Milky Way.

In retrospect, this should not be surprising because R136 is much different than a spiral galaxy. The bright, early-type stars in spiral galaxies are generally confined to relatively narrow galactocentric radii near that of their initial birth sites. In contrast, stars in elliptical galaxies similar to R136 undergo substantial mixing due to their highly eccentric orbits. Therefore, the form of the IMF in spirals could be different than that in R136.

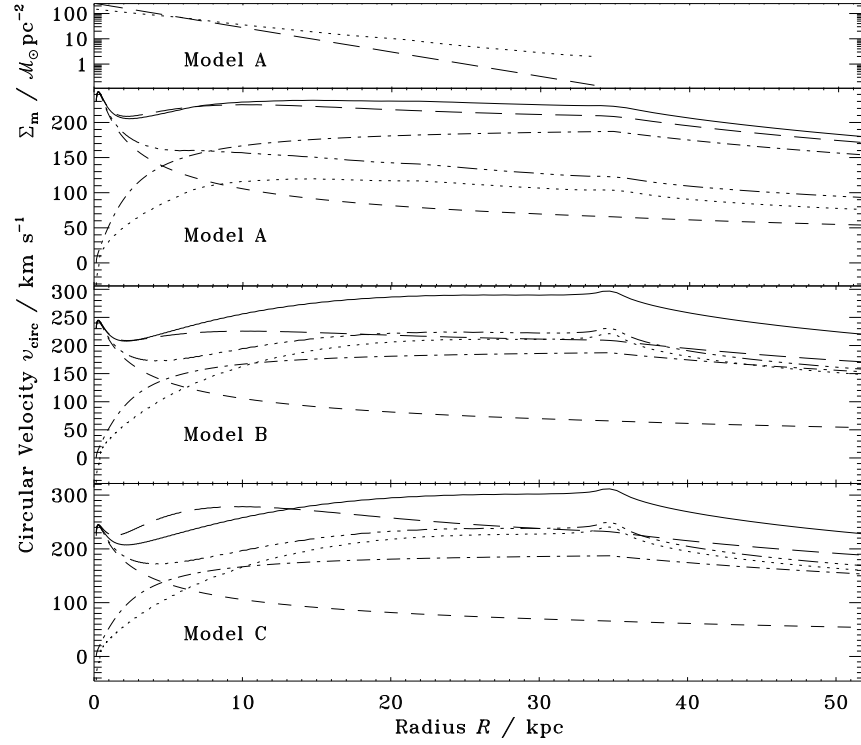


Fig. 1.— *Top panel*: the surface density of a spiral galaxy similar to the Milky Way but with the IMF of Model A. The dotted line is the surface density assuming that all stars lie on the main-sequence. The dashed line is the surface density if the V band mass to light ratio were constant at $\gamma_V = 2.0M_\odot/L_\odot$. *Lower three panels*: circular velocities of Models A (upper-middle), B (lower-middle), and C (bottom). The circular velocities of Model A correspond to the surface density function shown in the top panel. For each model, the solid curve accounts for all components of mass, the dot-dash curve accounts for just the halo, dotted curve accounts for just the disk, the short-dashed curve accounts for just the bulge and spheroid stars, the dash-dotted curve accounts for everything except the halo, and the long-dashed curve assumes that the mass to light ratio is constant at $\gamma_V = 2.0M_\odot/L_\odot$.

For this reason, other models were also considered. Model B was constructed in order to help answer the question of just how necessary the dark halo is for circular velocity curves to be flat. The IMF gradient Γ_1 was adjusted to minimize the curvature of the outer circular velocity curve, while Γ_0 was adjusted such that the rotation velocity was $\simeq 220 \text{ km s}^{-1}$. For simplicity, m_l and m_u were fixed. The middle plot of Figure 1 shows that the circular velocity curve of Model B is surprisingly flat throughout most of the outer regions of the disk before the halo component is included. The total disk mass for Model B is $2.4 \times 10^{11} M_\odot$, with $\langle \gamma_v \rangle_{\text{disk}} = 14.5 M_\odot / L_\odot$, which is 7.3 times larger than the $\gamma_v = 2.0 M_\odot / L_\odot$ model. The value of Γ_1 for Model B is 0.42. This is 50% higher than the IMF gradient in R136. The change within the Milky Way of Γ measured by Garmany et al. (1982) between the inner and outer semicircular regions of radius 2.5 kpc surrounding the Sun was -0.8, which for a disk scale length of $R_0 = 4.5 \text{ kpc}$ corresponds to $\Gamma_1 = 0.8 \times 3\pi R_0 / (8 \log e \times 2.5 \text{ kpc}) = 3.9$. This is much higher than the value in Model B. Thus the IMF gradient of Model B is well within empirical upper limits.

However, there are at least five potential problems with the halo-less form of Model B: **1)** In the adopted solar vicinity ($R_\odot = 7.8 \text{ kpc}$), the surface density is $179 M_\odot \text{ pc}^{-2}$. This is an unacceptable 15 standard deviations higher than the local value of $46 \pm 9 M_\odot \text{ pc}^{-2}$ measured by Kuijken & Gilmore (1989b). The corresponding mass to light ratio is $7.9 M_\odot / L_\odot$. This is 60% higher than the local value adopted in standard texts such as Binney & Tremaine (1987). Similarly, the IMF slope at this radius is $\Gamma = -1.7$. Also, for the low mass ($m \lesssim 0.5$) stars, this value is incompatible with Miller & Scalo's (1979) result of $\Gamma = -0.4$. **2)** Mestelian disks, which are similar to Model B, are commonly thought to be unstable to bar formation. The Toomre instability parameter Q is $\sigma_R \kappa / (2.9 G \Sigma_{\text{m}\odot})$, where $\kappa \simeq 36 \text{ km s}^{-1} \text{ kpc}^{-1}$ is the epicycle frequency and σ_R is the mass-weighted stellar velocity dispersion (Toomre 1974). Published estimates are $Q \simeq 1 - 3$ in the solar vicinity. Because stellar velocity dispersions are empirically observed to decrease with mass even for stars with lifetimes greater than the age of the galaxy, estimates of σ_R are sensitive to m_l . Wielen (1977) obtained $\sigma_R = 62 \pm 12 \text{ km s}^{-1}$ for $0.1 \lesssim m \lesssim 0.8 \text{ K and M dwarfs}$, which implies $Q \gtrsim 1.0 \pm 0.2$ for Model B. This lower limit is low enough to sustain spiral arm structure which numerical simulations show would rapidly dissipate otherwise. However, it is too near unity to prevent the growth of substantial arm/interarm stellar mass density contrasts. Though such mass contrasts are now known to exist in normal spirals (e.g., Rix & Zaritsky 1995, González & Graham 1996), they are not accounted for in Model B. Incidentally, the halo component does not necessarily affect this instability (Sellwood 1985). **3)** The circular velocity curve at $R \lesssim 35 \text{ kpc}$ is not precisely flat, but actually rises before attaining a nearly Keplerian fall off. This is the result of the non-spherical potential. **4)** The circular velocity drops below 200 km s^{-1} in the inner regions of the disk. This result is expected. For Model B, the mass to light ratio is $\simeq m_u^{1-y} (m_u/m_l)^{-\Gamma-1} (y + \Gamma) (M_\odot / L_\odot) / (-\Gamma - 1)$. If

$$\Gamma_1 = [\ln(m_u/m_l) \log_{10} e]^{-1}, \quad (1)$$

which Model B obeys to within 15%, the mass to light ratio would scale as $\simeq e^{R/R_0}$. This in turn would imply a disk surface density that is relatively constant. The circular velocities of such disks increase monotonically with R and are zero at $R = 0$. This problem with low inner disk velocities is

probably not serious because circular velocity curves are frequently compatible even with constant mass to light ratio, halo-less models throughout their entire optically-bright regions (e.g., Kent 1986). Furthermore, flatter, halo-less velocity curves could probably be attained by including the following: galaxy parameters slightly different than those of Kuijken & Gilmore (1989a), a (more realistic) log-normal IMF (Miller & Scalo 1979), expected spatial dependence in remnant and gas mass fractions, and variations of m_l or m_u with ρ_l . For instance, the velocity dip is better masked by the bulge if Bahcall & Soniera’s (1984) smaller disk scale length of 3.5 kpc is assumed. **5)** The IMF gradient of Model B appears to be too *small* to be compatible with the measurement of Garmany et al. (1982). Equation (1) suggests that this discrepancy would be less if a smaller m_u/m_l ratio had been employed.

Of the above potential problems, only the first two appear to be significant at this time. Both can be overcome by taking into account the arm/interarm density contrasts observed in spiral galaxies; Model C was constructed to be similar to Model B, but has an azimuthally-averaged light and mass density that is 3.25 times greater than the interarm values in which the Sun presumably resides. The circular velocity curve of Model C, shown in the lower panel of Figure 1, is slightly higher but otherwise similar to that of Model B. However, the solar-vicinity disk surface density is only $60M_\odot\text{pc}^{-2}$. This is a much more reasonable 1.6 standard deviations above the value determined by Kuijken & Gilmore (1989b) and is actually lower than Bahcall & Soniera’s (1984) value of $\simeq 85M_\odot\text{pc}^{-2}$.

4. DISCUSSION

A direct scaling of R136’s IMF to the Galaxy does not dramatically alter the circular velocity curve. However, Models B and C, with their higher yet modest IMF gradients, have nearly flat $v_{\text{circ}} \lesssim 220 \text{ km s}^{-1}$ circular velocity curves only before the traditional dark halo component is included. It is interesting to note that if one assumes that these types of models and their $\sim 10^1$ -fold mass enhancements are representative of most galaxies, that the fiducial stellar contribution towards the closure density is $\Omega_* \simeq 0.004$ (e.g., Peebles 1993) before accounting for IMF gradients, that the cosmological constant is zero, and that there is no hot dark matter, one would obtain $\Omega \simeq \Omega_{\text{baryon}} \simeq 0.04 + \Omega_{\text{gas}}$, where the closure fraction due to all gas including hot plasma in galactic clusters is $0.007 \lesssim \Omega_{\text{gas}} \lesssim 0.08$ (Mulchaey et al. 1996).

Current models of galactic evolution (e.g., Worthey 1994, de Jong 1996) do not account for IMFs that might vary with time and position via the temperature. This is despite prior warnings that the IMF probably has important dependences upon time and position (e.g., Mihalas & Binney 1978). In light of the above results, accounting for IMFs with such dependences may be necessary even to obtain results that are only accurate to first order. Accounting for these dependences may, for relatively obvious reasons, clarify our understanding of several astrophysical phenomena including the G-dwarf problem, intrinsic (as a function of radius) and extrinsic (as a function of

galactic morphology) metallicity and color gradients, and the Tully-Fisher relation.

It is my pleasure to thank M. Harris, F. Bruhweiler, A. Whiting, A. Fridman, D. Kazanas, D. Audley, J. Knapen, A. Mignogna, E. Albert, and A. Stupp for useful comments. This work is part of a dissertation to be submitted to the Graduate School, University of Maryland in partial fulfillment of the requirements of the Ph.D. degree in Physics.

REFERENCES

- Adams, F., & Fatuzzo, M. 1996, *ApJ*, 464, 256
- van Albada, T. S., Bahcall, J. N., Begeman, K., & Sancisi, R. 1985, *ApJ*, 295, 305
- Augarde, R., & Lequeux, J. 1985, *A&A*, 147, 273
- Bahcall, J. N. & Soniera, R. M. 1984, *ApJS*, 55, 67
- Binney, J., & Tremaine, S. 1987, *Galactic Dynamics* (Princeton: Princeton University Press)
- Bodenheimer, P., Tohline, J. E., & Black, D. C. 1980, *ApJ*, 242, 209
- Brandl, B., et al. 1996, *ApJ*, 466, 254
- Campbell, B., et al. 1992, *AJ*, 104, 1721
- Doane, J. S., & Mathews, W. G. 1993, *ApJ*, 419, 573
- Doyon, R., Joseph, R. D., & Wright, G. S. 1994, *ApJ*, 421, 101
- Edmunds, M. G., & Phillipps, S. 1989, *MNRAS*, 241, 9
- Garmany, C. D., Conti, P. S., & Chiosi, C. 1982, *ApJ*, 263, 777
- González, R. A., & Graham, J. R. 1996, *ApJ*, 460, 651
- Humphreys, R. M., & McElroy, D. B. 1984, *ApJ*, 284, 565
- Hunter, D. A., et al. 1996, *ApJ*, 459, L27
- Kent, S. M. 1986, *AJ*, 91, 1301
- Kuijken, K., & Gilmore, G. 1989a, *MNRAS*, 239, 571
- Kuijken, K., & Gilmore, G. 1989b, *MNRAS*, 239, 605
- de Jong, R. S. 1996, *A&A*, 313, 377
- Larson, R. B. 1982, *MNRAS*, 200, 159
- Malumuth, E. M., & Heap, S. R. 1994, *AJ*, 107, 1054
- Miller, G. E., & Scalo, J. M. 1979, *ApJS*, 41, 513
- Mulchaey, J. S., Davis, D. S., Mushotzky, R. F., & Burstein, D. 1996, *ApJ*, 456, 80

- Padoan, P., Nordlund, A., & Jones, B. J. T. 1997, MNRAS, 288, 145
- Peebles, P. J. 1993, Principles of Physical Cosmology (Princeton: Princeton University Press)
- Phillipps, S., Edmunds, M. G., Davies, J. I. 1990, MNRAS, 244, 168
- Rieke, G. H., Lebofsky, M. J., Thompson, R. I., Low, F. J., & Tokunaga, A. T. 1980, ApJ, 238, 24
- Rix, H., & Zaritsky, D. 1995, ApJ, 447, 82
- Salpeter, E. E. 1955, ApJ, 121, 161
- Schaller, G., Schaerer D., Mynet G., & Maeder A. 1992, A&AS, 96, 269
- Sellwood, J. A. 1985, MNRAS, 217, 127
- Toomre, A. 1974, in Highlights of Astronomy, ed. G. Contopoulos (Dordrecht: Reidel), 457
- Wielen, R. 1977, A&A, 60, 263
- Worthey, G. 1994, ApJS, 95, 107

Table 1: IMFs in R136

R/pc	$\Gamma(R)$	m_l	m_u	$\rho_l/(L_\odot\text{pc}^{-3})$
0.20	-1.29 ± 0.20	5.6	120	1.5×10^6
0.60	-1.46 ± 0.23	3.6	76	1.5×10^5
2.0	-2.12 ± 0.09	≤ 2.0	48	1.5×10^3

Note. — Data adapted from Brandl et al. (1996) for (age-spread restricted) stars 2.5–3.5 Myr old.

Table 2: Model Parameters

Model	Γ_0	Γ_1	m_{l0}	m_{l1}	m_{u0}	m_{u1}	$\rho_{m\odot}/M_\odot\text{pc}^{-3}$	$\Sigma_{m\odot}/M_\odot\text{pc}^{-2}$	$\langle \Sigma_{m\odot} \rangle / M_\odot\text{pc}^{-2}$
A	-3.03 (± 0.26)	0.28 (± 0.06)	-0.08	0.13	1.25 (± 0.23)	0.12 (± 0.04)	0.12	67	67
B	-1.11	0.42	-1.52	0.00	1.30	0.00	0.31	179	179
C	-0.55	0.40	-1.52	0.00	1.60	0.00	0.10	60	195

Note. — This assumes $f = f_0 + f_1 \log_{10}[\rho_l/(L_\odot\text{pc}^{-3})]$, for $f = \Gamma, \log_{10}(m_l)$, or $\log_{10}(m_u)$.